Journal of Medicinal Chemistry

Drug Annotation

Discovery, pharmacokinetic and pharmacological properties of the potent and selective MET kinase inhibitor, 1-{6-[6-(4-Fluoro-phenyl)-[1,2,4]triazolo[4,3-b]pyridazin-3-ylsulfanyl]-benzothiazol-2-yl}-3-(2-morpholin-4-yl-ethyl)-urea (SAR125844)

Antonio Ugolini, Mireille Kenigsberg, Alexey Rak, François Vallée, Jacques Houtmann, Maryse Lowinski, Cécile Capdevila, Jean Khider, Eva Albert, Nathalie Martinet, Conception Nemecek, Sandrine Grapinet, Eric Bacqué, Manfred Roesner, Christine Delaisi, Loreley Calvet, Fabrice Bonche, Dorothée Semiond, Coumaran Egile, Hélène Goulaouic, and Laurent Schio

J. Med. Chem., **Just Accepted Manuscript** • DOI: 10.1021/acs.jmedchem.6b00280 • Publication Date (Web): 29 Jun 2016

Just Accepted

ACS Publications

Journal of Medicinal Chemistry is published by the American Chemical Society. 1155 Sixteenth Street N.W., Washington, DC 20036

Discovery, pharmacokinetic and pharmacological properties of the potent and selective MET kinase inhibitor, 1-{6-[6-(4-Fluoro-phenyl)-[1,2,4]triazolo[4,3-b]pyridazin-3-ylsulfanyl]-benzothiazol-2-yl}-3-(2-morpholin-4-yl-ethyl)-urea (SAR125844)

Antonio Ugolini,[†] Mireille Kenigsberg, [¶] Alexey Rak, [‡] Francois Vallée,[‡] Jacques Houtmann,[‡] Maryse Lowinski,[‡] Cécile Capdevila, [µ] Jean Khider,[†] Eva Albert,[†] Nathalie Martinet,[†] Conception Nemecek,[†] Sandrine Grapinet,[†] Eric Bacqué,[†,ϕ] Manfred Roesner, [ł] Christine Delaisi,[¶] Loreley Calvet, [¶] Fabrice Bonche, [†] Dorothée Semiond, [†,ƽ] Coumaran Egile,[¶,§] Hélène Goulaouic, [¶] Laurent Schio[†,]*

[†]Medicinal Chemistry, [¶]Oncology Drug Discovery, [‡] Structure Design & Informatics, [µ] Protein Science & Technology, Sanofi, 13 quai Jules Guesde, 94403 Vitry-sur-Seine, France. [†]Disposition Safety Animal Research, 1 avenue Pierre Brossolette, 91385 Chilly-Mazarin, France. [ł]Industriepark Hoechst, 65926 Frankfurt am Main, Germany.

Current address: [§]AstraZeneca, Oncology Innovative Medicines, Personalized Healthcare and Biomarkers, United Kingdom; [ϕ] Infectious Diseases Unit, 1541 Avenue Marcel Merieux, 69280, Marcy L'Etoile, France; [ƽ] 500 Kendall St, 2142 Cambridge, MA, United States.

ABSTRACT: The HGF/MET pathway is frequently activated in a variety of cancer types. Several selective small molecule inhibitors of the MET kinase are currently in clinical evaluation, in particular

for NSCLC, liver and gastric cancer patients. We report herein the discovery of a series of triazolopyridazines that are selective inhibitors of wild-type (WT) MET kinase and several clinically relevant mutants. We provide insight into their mode of binding and report unprecedented crystal structures of the Y1230H variant. A multi-parametric chemical optimization approach allowed the identification of compound **12** (SAR125844) as a development candidate. In this chemical series, absence of CYP3A4 inhibition was obtained at the expense of satisfactory oral absorption. Compound **12**, a promising parenteral agent for the treatment of MET-dependent cancers, promoted sustained target engagement at tolerated doses in a human xenograft tumor model. Preclinical pharmacokinetics conducted in several species were predictive for the observed pharmacokinetic behavior of **12** in patients.

KEYWORDS: c-Met, MET kinase inhibitor, *MET* amplification, SAR125844, triazolopyridazine, multi-parametric optimization, Y1230H X-ray structure.

The MET receptor tyrosine kinase is activated by binding of its ligand, Hepatocyte Growth Factor (HGF), resulting in receptor dimerization, auto-phosphorylation of Tyr1234/1235, activation of the kinase domain and of the downstream multiple signaling pathways, including RAS/MAPK and PI3K/AKT, which in turn promote cell proliferation, survival, motility, invasion, angiogenesis and morphogenesis.[1,2] The HGF/MET pathway plays an essential physiological role during embryogenesis[3], and a more restricted role in tissue regeneration and damage repair in healthy adults.[4,5] Dysregulation of MET has been reported in several tumor types, either in the form of overexpression of the MET receptor, or as mutations[6, 7] and amplification[8] of the *MET* gene. Importantly, *MET* gene amplification was reported as an acquired resistance mechanism to EGFR tyrosine kinase inhibitor therapies in 10-20% of Non-Small Cell Lung Cancer (NSCLC) patients[9,10,11] and to anti-EGFR monoclonal antibody treatment in Colorectal Cancer (CRC) patients.[12] More recently, HGF expression in the tumor stroma was reported as a resistance mechanism to BRAF inhibitors.[13]

Several orally bioavailable MET tyrosine kinase inhibitors, including Capmatinib (INC280),[14] Tepotinib (EMD1214063),[15] Savolitinib (Volitinib/AZD6094/HMPL-504),[16] (R)-6-(1-(8-Fluoro-6-(1-methyl-1H-pyrazol-4-yl)-[1,2,4]triazolo[4,3-a]pyridin-3-yl)ethyl)-3-(2-methoxyethoxy)-1,6-naphthyridin-5(6H)-one (AMG-337)[17] as well as the MET/ALK/ROS inhibitor Crizotinib,[18] are in Phase II clinical trials in papillary renal cell carcinoma, NSCLC, gastro-esophageal and hepatocellular cancer. We report here the discovery, pharmacological characterization, preclinical and clinical pharmacokinetics of 1-{6-[6-(4-Fluoro-phenyl)-[1,2,4]triazolo[4,3-b]pyridazin-3-ylsulfanyl]-benzothiazol-2-yl}-3-(2-morpholin-4-yl-ethyl)-urea, compound **12** (SAR125844), a potent intravenously active and highly selective MET kinase inhibitor; comparable to the aforementioned MET specific clinical candidates as assessed through biochemical and cellular profiling.[19, 20]

The original hit identification approach was based on a medium-throughput screening of an in-house biased kinase inhibitor library tested in a biochemical assay using non-phosphorylated MET kinase domain in order to identify all classes (DFG in (Asp-Phe-Gly), DFG out, α-Helix out etc.) of potential inhibitors.[21] Subsequent biochemical assays were performed with phosphorylated MET kinase domain during the optimization phase.

A set of benzimidazole sulfonate derivatives with nanomolar MET inhibition was identified. In particular, the initial hit **1** (Figure 1) exhibited an IC_{50} of 5 nM against MET kinase but also displayed a strong undesirable affinity for Cyclin Dependent Kinase CDK9 (IC_{50}= 6 nM), an isoform involved in gene transcription processes. Modification of the sulfonyl aryl moiety with more bulky substituents (e.g. chlorine vs fluorine atoms in analog **2**) was well tolerated in the MET protein (**2**: MET IC_{50} = 23 nM) and resulted in prohibitive steric clashes and reduced binding to CDK9 (**2**: IC_{50}= 1200 nM). However, compound **2** also displayed potent tubulin affinity (IC_{50} = 2.7 μM, and microtubule poisons are active in the 0.5-3 μM sub-stoichiometric concentration range in a microtubule assembly assay performed with 6-8 μM tubulin) leading to off-target cytotoxicity in non-MET-dependent tumor cell lines.

Revisiting the internal compound collection retrieved a set of about 2000 benzimidazole derivatives from which a potent singleton originating from a former anthelmintic program was identified by testing on the phosphorylated MET kinase domain. Triazolopyridazine **3** was active (IC_{50} = 10 nM) in the MET biochemical assay, the ELISA P-MET cell-based assay as well as the proliferation assay using the MKN-45 *MET*-amplified gastric tumor cell line. Compound **3** was inactive on CDK9 (IC_{50} > 10 μM) but still displayed affinity toward tubulin (IC_{50} = 2 μM).

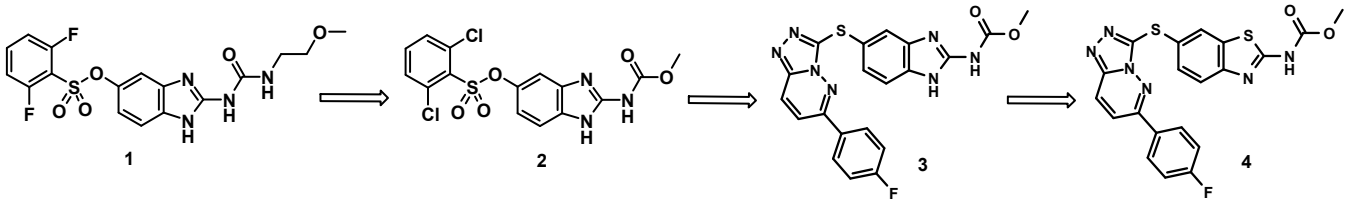

Figure 1. Hit and lead finding steps

To unravel the molecular interactions responsible for the kinase activity observed we initiated structural characterization of compound **3** bound to the WT MET kinase domain**.** Co-crystals were grown, X-ray diffraction data collected (1.6Å resolution at the ESRF synchrotron ID 14-2 beamline in Grenoble, France) and the 3D structure of the complex determined. Structure analysis revealed that compound **3** binds to the kinase ATP pocket, forming two H-bonds with the hinge region (Met1160, Figure 2A). In addition, one of the nitrogen atoms of the triazolopyridazine moiety interacts with the main-chain nitrogen atom of Asp1222. The triazolopyridazine ring makes a π-π interaction with Tyr1230 of the activation loop positioned in a non-active conformation. This binding mode is a structural feature of the so-called type I inhibitors, as exemplified by Crizotinib and other triazolopyridazine / triazolopyridine-bearing MET inhibitors.[22]

Based on the co-crystal structure of **3** bound to MET kinase, chemical modifications were designed and performed to simultaneously improve (i) the potency against WT MET and MET mutant proteins, (ii) the selectivity (among kinases and *vs* tubulin) and (iii) the aqueous thermodynamic solubility. The latter physicochemical property was assessed under two conditions, in pure buffer (intrinsic solubility) and

with a co-solvent (labrasol) as a preliminary formulation. In the course of the optimization program the benzothiazole sub-series (e.g. compound **4**, Figure 1 and Table 1) stood out as more attractive than the corresponding benzimidazoles, since it was not binding to tubulin (IC_{50} > 25µM) and had no Ames alert (compound **3** was found Ames positive). However, switching to the benzothiazole series was at risk from a druggability standpoint as compound **4** was more lipophilic compared to **3** (logD = 4.6 versus 3.8) and exhibited decreased aqueous solubility in the conditions tested.

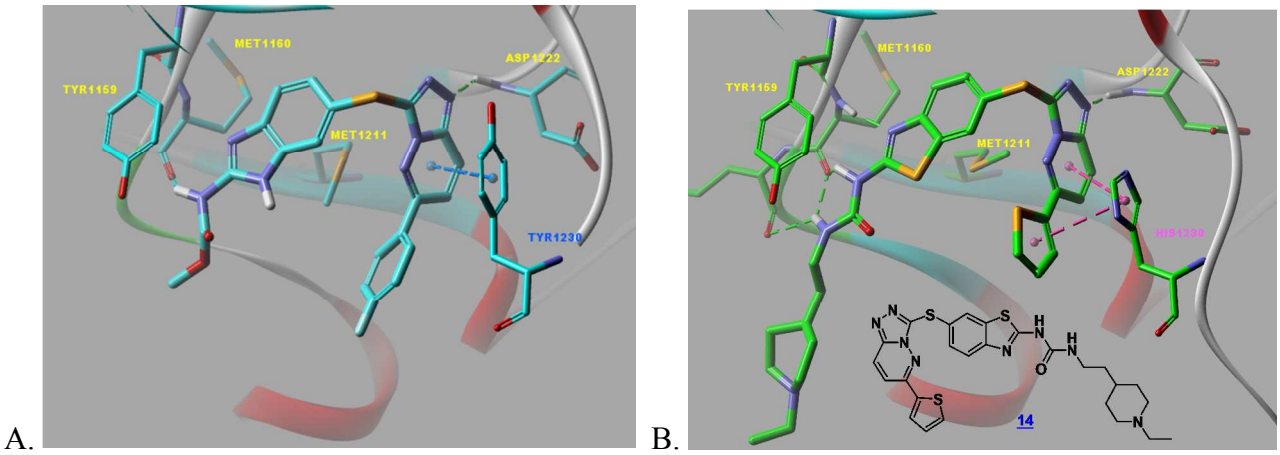

Figure 2. X-ray structures of WT MET with **3** (A) and MET-Y1230H with **14** (B)

Various chemical moieties (carbamates, amines, amides and ureas) were introduced in position 2 of the benzothiazole scaffold allowing at least a double interaction with the hinge region of the kinase (R1 group in Table 1). Most of the modifications depicted in Table 1 were well tolerated leading to potent kinase inhibitions in the biochemical assay, which consistently translated into significant P-MET inhibition in the cell-based assay, as well as anti-proliferative activity on the *MET*-amplified MKN-45 cell line (IC_{50} values of 10-100 nM). Although these compounds were found to be significantly active against the M1250T mutant, they revealed to be less potent when considering L1195V and Y1230H mutants (see compounds **4**, **5**, **6** &**7** vs **8** and **9** in Table 1). Interestingly, the most catalytically active mutants were also the most sensitive ones (data not shown). In addition sub-micromolar inhibition of the Y1230H mutant was achieved only with compounds that were active at least in the nanomolar range against WT MET protein (compounds **9**, **12** & **13**). From a structure-potency relationship point of view, introduction of a third interaction between the additional nitrogen atom brought by the urea group and

the hinge does not explain the observed gain of activity for ureas **12** and **13** (compared to **4**) since cyclopropyl amide **9** is equipotent to ureas **12** and **13**. To better understand the thermodynamics of binding in the selected series, we performed Isothermal Titration Calorimetry (ITC) measurements[23] with a series of analogs including the most active compound **12**. In general, a good correlation was observed between the biochemical IC_{50} and the Kd obtained by calorimetry (e.g. Kd = 0.9 nM vs IC_{50} = 4nM for **12**). The free energy of binding of compound **12** to the WT protein was measured experimentally and found to be totally driven by the enthalpy contribution ($\Delta G=\Delta H=$ -12.6 Kcal/mol), a trend shared by the different triazolopyridazine compounds tested and in contrast to the ITC profile of Crizotinib (Figure 3).

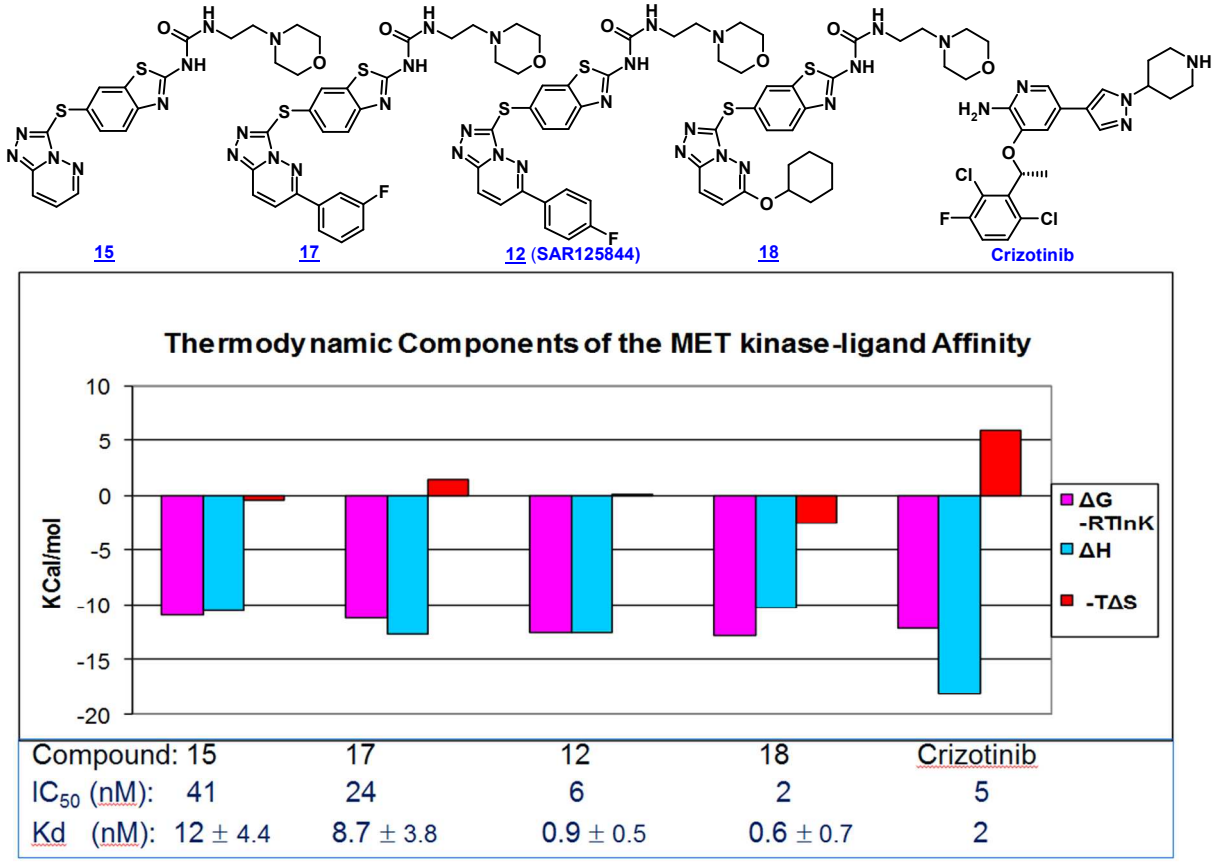

Figure 3: Structures of key compounds with biochemical and ITC data.

This raised the hypothesis that potency was directly dependent on the number of hydrogen bonds, Van der Waals interactions and hydrophobic contacts[24] the inhibitor could establish with the protein. To gain insight on improving the affinity for MET mutants, co-crystallization attempts with compound **12** were performed on Y1230H, L1195V and M1250T mutant proteins, and with MET WT as well**.** Surprisingly,

whereas the WT protein did not yield any crystals, 3D structures were readily obtained with the different MET mutants. Structural analysis of different complexes with **12** revealed 4 conserved major hydrogen bonds, three developed with Met1160 and Lys1161 of the hinge and one with Asp1222 of the DFG motif.

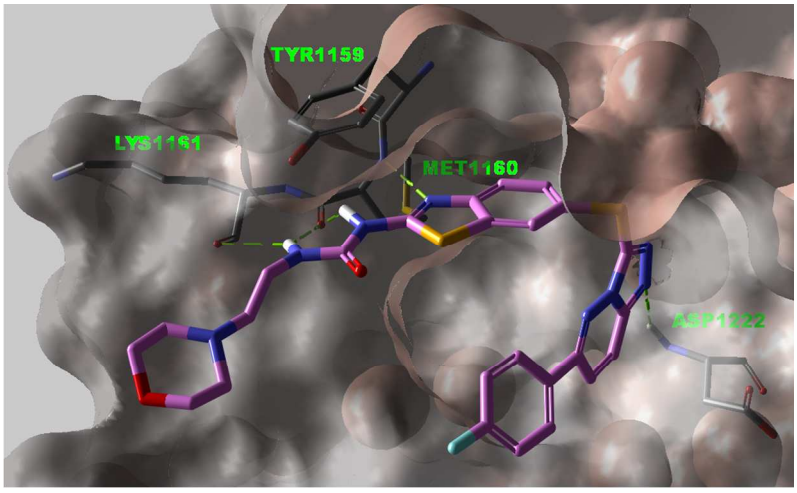

Figure 4: Crystal structure of **12** in the Y1230H mutant showing the tight interaction with the hinge and the DFG Asp1222.

On the other hand, the activation loop segment containing residue 1230 was not visible in any structure with **12** (supplementary information). Similarly to the 3D structure of **3** in WT MET protein, the mutated proteins were locked in a DFG in, α-C helix out conformation with a disrupted salt bridge between catalytic Lys1110 and α-C Helix Glu1127[25]. Non-visibility of the H1230 residue bearing segment in the MET Y1230H co-crystal structure raised the question whether reduced affinity of compound **12** (and other analogs) for this mutant might be linked to a sub-optimal π-π interaction of the triazolopyridazine core with the imidazole ring of H1230. This hypothesis was confirmed when compound **14** (analog of **12**) was successfully co-crystallized in the MET Y1230H mutant, the structure of the complex showing a clear positioning of the histidine residue in the electron density maps (Figure 2B). In this crystal structure, the triazolopyridazine plane is twisted outward by ~20° with respect to other analogs, thus placing the thiophene ring roughly parallel to H1230. Also observed is a slight shift of H1230 (~1Å) towards the solvent compared to Y1230 as seen in other WT MET structures. High potency of **14** against MET Y1230H mutant (IC_{50} = 23 nM) could then be explained by favorable

hydrophobic contacts between H1230 and the triazolopyridazine-thiophene segment (extended π-system). This hydrophobic interaction is likely enhanced by the planarity of the triazolopyridazine-thiophene segment whereas the skewed nature of the triazolopyridazine-p-fluorophenyl observed in **3** probably also precludes a productive contact in **12** (supplementary information).

Table 1. Biochemical and cellular activities on wild-type MET, biochemical activity on MET mutants, and aqueous solubility of benzothiazole derivatives **4-14**

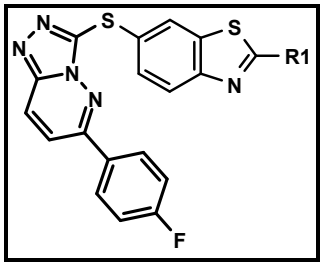

Compound	R1	P-MET WT IC_{50} (nM)[a]	ELISA P-MET IC_{50} (nM)[b]	MKN-45 Proliferation IC_{50} (nM)[c]	L1195V IC_{50} (nM)[d]	M1250T IC_{50} (nM)[d]	Y1230H IC_{50} (nM)[d]	logD (pH7.4)[e]	Aqueous Solubility (µM, pH7.4)[f]		Ref.[g]
										+10% Labrasol	
4	$NHCO_2Me$	16	22	91	>10000	nd	>10000	>4.6	<1	15	26
5	NH_2	10	43	81	9000	245	>10000	>4.6	nd	44	26
6	NHEt	15	15	42	>10000	417	>10000	>4.6	<2.5	nd	
7	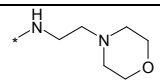	20	13	45	835	455	>10000	4.1	<1	543	26
8	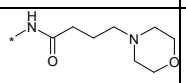	6	2	12	318	93	1172	4.3	nd	96	26
9	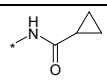	3	4	7	61	13	883	4.7*	<1	64	26
10	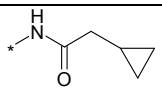	4	13	22	>10000	128	>10000	>4.6	<2	nd	
11	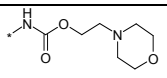	45	25	95	6523	nd	>10000	4.1	8	245	26
12	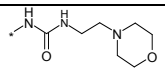	4	5	7	64	6	204	4.2	<1	500	26
13	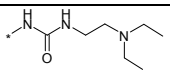	3	10	33	148	71	864	4.15	<1	1000	26
14	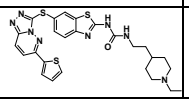	2	29	2.7	nd	nd	23	3.9	<2	nd	

[a] *IC_{50} measured using phosphorylated protein in a biochemical assay*

[b] *IC_{50} for cell-based P-MET, using an ELISA assay and MKN-45 cell line*

[c] *IC_{50} measured in proliferation assay using MKN-45 cell line*

[d] *IC50 measured using MET mutants in a biochemical assay*

see Supporting Information for details on assays [a, b, c, d]

[e] *Measured experimentally by High Performance Liquid Chromatography (HPLC) (Xterra MS C18 column)*

[f] *Equilibrated solubility measured in phosphate buffer with and without 10% labrasol*

[g] *Compounds were prepared according to the methods in the reference cited*

This observation prompted us to initiate a second round of chemical optimization with modifications of the substituent linked to the triazolopyridazine core. The main purpose was to identify alternative replacements of the thiophene and significantly improve the aqueous solubility. The reported activities and drug like properties (solubility, permeability in Caco-2 cells, metabolic stability on human microsomes, reversible and irreversible inhibition of CYP3A4) are shown in Table 2.

Compared to compound **15** (R2 = H), most of the substituents that were introduced led to potent analogs against the WT MET protein; having variable activity against the MET Y1230H mutant. The lack of permeability observed in the Caco-2 assay (Table 2) could be attributed to several unfavorable factors like high molecular weight (in general around 550 g/mol), high number of H-bond acceptors (at least 10 as in **15**) and low intrinsic aqueous solubility; in spite of the balanced morpholino group basicity (pka = 6.5) suitable for passive diffusion.[27] In contrast, 6-O-alky analogs showed good to moderate Caco-2 permeability (compounds **18**, **23** & **24**). It remained unclear how to rationalize this observation since these molecules exceed molecular weight (MW) of 500 g/mol, display 11 H-bond acceptors and besides **13** and **26** the highest number of rotatable bonds (7) of this set of compounds.[28] In line with the Caco-2 results, compounds **18** and **23** exhibited moderate bioavailability in mouse PK studies (17% and 12%, respectively) as observed finally with many other *extended rule of 5* (Ro5) compliant molecules.[29] Unfortunately, these molecules were discarded due to their inhibitory activity on the CYP3A4 isoform in a time-dependent manner (mechanism-based inhibition). Overall, taking into account the properties of R2 derivatives reported in Table 2, compound **12** turned out to be the best compromise in terms of potency and drug-like properties in particular regarding CYP450 inhibition. In the end, attempts to improve solubility in this chemical series failed as key atoms interacting with the MET proteins also

proved to be involved in strong packing forces in compound solid states. The single crystal X-ray structure (Figure 5) of one polymorph of **12** attested to the dense packing of this solid state. The two flat conjugated pi-systems disposed in a right angle configuration by the sulfur linker displayed stabilizing H-bond, lipophilic and π-stacking interactions (supplementary materials).

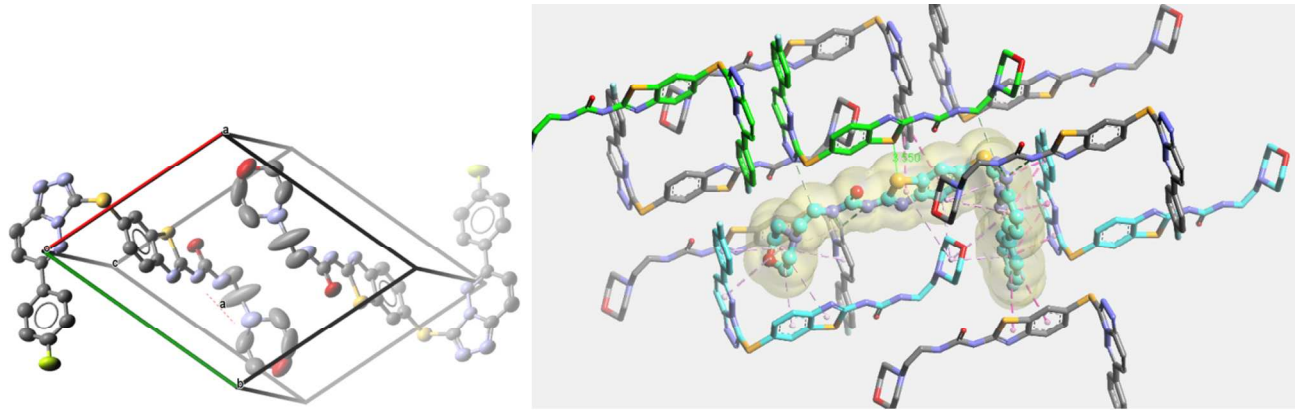

Figure 5: Unit cell and packing views in the X-ray single crystal diffraction structure of **12**

In PK studies in mice, the oral bioavailability of **12** was low (~2%) in line with its moderate Caco-2 permeability. Hence, **12** was progressed toward *in vivo* preclinical studies as a parenteral agent for the treatment of MET-dependent cancer.

Table 2. Multi-parametric analysis of morpholino ethyl urea analogs[26, 30]

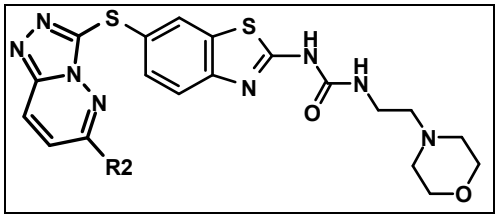

Compound	R2	P-MET WT IC_{50} (nM) [a]	P-MET Y1230H IC_{50} (nM) [b]	aqueous solubility pH7.4 (µM) [c]		Permea-bility in Caco-2 cells [d]	% metabol. in human micro-some [e]	Inhibition of CYP3A4 (IC_{50}, µM) [f]	CYP3A4 inhibition (MBI) [g]	Ref. [h]
				Aq. buffer	Labrasol					
15	H	29	4805	70	1070	0	11	34	-2.3	26

12	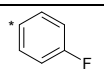	4	204	<2	500	9	23	>200	No*	26
16	OEt	3	643	5	460	0	51	4	-13.1	26
17		10	140	32	1170	4	24	1.8	-8.2	26
18	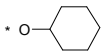	2	252	<2	500	98	23	2.7	-4.6	30a
19	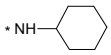	1	139	<2	ND	0	38	2.9	-9.1	30a
20	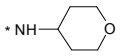	1	217	89	ND	2	39	>40	-14.2	30c
21		1	274	<2	ND	0	26	0.2	-3.8	30a
22	OPh	2	174	<2	ND	8	32	7.9	-12.8	30b
23	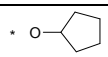	6	216	<2	ND	26	29	31	-5.5	30a
24	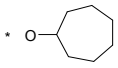	15	407	<2	ND	20	36	14	-11.6	30a
25	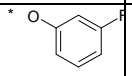	3	56	<2	ND	8	16	2	-12.2	30b
26	O-nBu	5	140	<2	ND	7	23	8.7	-11.3	

[a] *IC_{50} measured using pre-phosphorylated wild-type MET kinase domain in a biochemical assay*

[b] *IC50 measured using MET mutant Y1230H in a biochemical assay*

[c] *Equilibrated solubility measured in phosphate buffer with and without 10% labrasol*

[d] *Trans-Epithelial Transport across Caco-2/ TC-7 Monolayers (Papp = 10^{-7} cm.sec-1)*

[e] *Percentage of oxidative metabolism using Hepatic Microsomal Fraction (20 minutes incubation, 1 mg/mL microsomes,5μM substrate)*

[f] *IC50 measured using recombinant human CYP3A4 with 7-benzyloxyquinoline as substrate*

[g] *Negative Slope values in %/min reflect potency of the Mechanism-Based Inhibition*

[h] *Compounds were prepared according to the methods in the references cited*

See Supporting Information for details on assays [a, b, d, e, f]

** for IC50 higher than 100 μM, no slopes can be determined and is defined as not quantifiable*

The pharmacokinetic and pharmacodynamic properties of compound **12** were first documented in female SCID mice bearing xenograft tumors based on the *MET*-amplified Hs 746T human gastric tumor cell line. To this end, a single intravenous administration at 20 mg/kg was performed. Compound **12** concentration was measured in both plasma and tumor tissue. The plasma exposure of **12** (Area Under the Curve (AUC)) was 6190 h.ng/mL, the clearance moderate (CL = 3.1 L/h/kg) and the volume of distribution was large (V_{ss} = 4.2 L/kg). A rapid and sustained uptake of **12** in tumor tissue was observed, associated with a slower decrease of compound **12** concentration from tumor tissue compared to the plasma concentration. These results indicate a higher tumor to plasma exposure of **12** (with a tumor to plasma AUC ratio equal to 8.1; Figure 6A).

Pharmacodynamic analysis in tumor tissue demonstrated a time-dependent reduction of MET kinase activity. Following administration of **12** at 20 mg/kg , phospho-MET(Y1349) evaluation in tumor extracts revealed that MET kinase inhibition was complete at 4 hours (96%), significant at 24 hours (80%) and partial at 48 hours (61%) (Figure 6B). A direct relationship was observed between PD modulation and tumor concentration of **12** rather than with plasma concentration in this murine model. Significant P-MET inhibition at 24h was associated with compound concentration of about 300 ng/ml in the tumor which represented an unbound drug exposure of about 2nM above the IC_{50} estimated in vitro vs Hs 746T cell lines (1 nM). It is worth mentioning that high protein binding of **12** in plasma (99.67%) did not prevent the molecule from distributing to the tumor tissue. This pharmacodynamic impact translated into tumor regression, as previously described.[20]

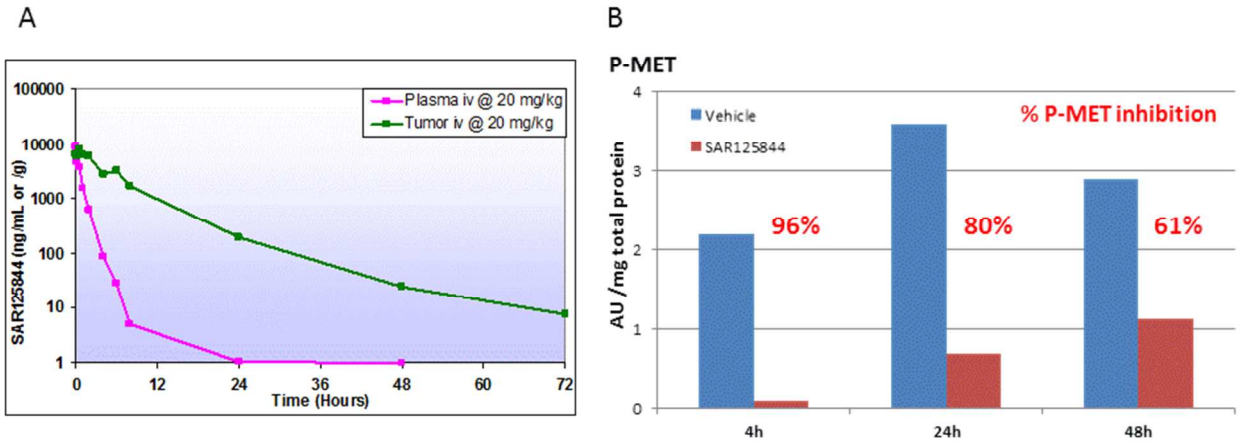

Figure 6: Pharmacokinetic/Pharmacodynamic (PK/PD) study of compound **12** in mice bearing xenograft tumor of the *MET*-amplified Hs 746T human gastric tumor cell line. Mice bearing established subcutaneous tumors derived from Hs 746T gastric cancer cell line were administered a single 20 mg/kg dose of **12** IV in the tail vein. The pharmacokinetic parameters of **12** were assessed by analysis of the drug concentrations in plasma and tumor tissue (A). The pharmacodynamic effect on MET kinase was assessed by analysis of phospho-MET(Y1349) levels in tumor extracts using Meso Scale Discovery (MSD) immunoassay (B).

The PK parameters of **12** were further characterized at lower intravenous doses in mice, rats and dogs (Table 3). In all 3 species evaluated the clearance was moderate. The plasma terminal elimination half-life ($t_{1/2}$) was moderate (rats and dogs) to long (mice). The volume of distribution at steady state was moderate in dogs and large in rodents. The potential large tissue distribution in rodents was further confirmed by performing a tissue distribution study in rats, with an infusion of 25 mg/kg [^{14}C]-**12**. Radioactivity was widely distributed throughout the whole body with maximum radioactivity concentrations reached in most tissues at the end of the infusion (i.e., 1 hour) or 2 hours after the start of infusion. Taken together, these results indicate a large distribution into the tumor tissue.

Table 3. Main PK parameters of **12** given IV in pre-clinical models

Parameter[a]	***Mouse***	***Rat***	***Dog***
Dose, mg/kg (IV)	1	5	3
CL (L/h/kg)[b]	2.8	1.5	0.5
CL as % of blood flow	54	36	20
Vss (L/kg)	3.2	2.9	1.3
$t_{1/2}$ (h)	4.8	3.6	3.8

[a] Mean PK parameters in 3 female (mice and dogs) or male (rats) animals
[b] Plasma CL for animal species (blood /plasma ratio = 0.86)

Preliminary PK analysis from the Phase I clinical trial[31] indicated that compound **12** blood exposure (AUC) increased proportionally from 50 to 740 mg/m². After the first administration, the concentrations decreased over time with a terminal half-life of 15.9 hours. Compound **12** exhibited a medium blood clearance (mean 33.9 L/h corresponding to approximately 0.5 L/h/kg, coefficient of variation (CV) 38%), representing approximately 37% of the hepatic blood flow (87 L/h) and a large volume of distribution at steady state (mean 505 L corresponding to approximately 7.2 L/kg, CV 99%). Taken together, the disposition of **12** was assessed in a range of animal species, and the distribution and elimination processes documented in animals are consistent with the disposition observed in humans. Thus, the animal pharmacological models tested were likely to be predictive for efficacy of **12** in patients.

In conclusion, the chemical optimization of a focused-screen hit, supported by structural analysis, led to the identification of compound **12**, a very potent and selective MET kinase inhibitor with favorable druggability properties for intravenous administration, and sustained target engagement in a *MET*-amplified tumor model. Overall, the compound profile being compatible with a weekly schedule of administration, further development with IV route was initiated, since some patients (e.g. MET-amplified esophagogastric adenocarcinoma) could prefer an IV infusion to an oral tablet. It is also possible that a less frequent dosing (weekly) versus a repeated format (daily) would trigger less acquired resistance to such treatment. A favorable tolerance profile was observed in Phase I patients, with a dose escalation performed up to the MAD of 740 mg/m^2 (MTD 570 mg/m^2). Early evidence of antitumor activity triggered the evaluation of compound **12** in a Phase II clinical trial in *MET*-amplified NSCLC patients (NCT02435121).

ASSOCIATED CONTENT

Supporting Information

3D views presented here were generated using BIOVIA Discovery Studio 4.5/2016 software and Cambridge Crystallographic Data Centre Mercury CFC 3.7. The atomic coordinates and structure

factors have been deposited in the Protein Data Bank, www.pdb.org; PDB ID codes: 5HLW (**cpd 14**), 5HNI (**cpd 3**), 5HO6 (**SAR125844**-Y1230H), 5HOA (**SAR125844**-L1195V) and 5HOR (**SAR125844**-M1250T).

AUTHOR INFORMATION

Corresponding Author

* E-mail: laurent.schio@sanofi.com. Phone: +33(0)1 58 93 88 14.

Present Address

13 Quai Jules Guesde, 94403 Vitry-sur-Seine Cedex, France

Notes

The authors declare no competing financial interest.

ACKNOWLEDGMENTS

This article is dedicated to the memory of our colleagues Jean-Yves Crenne[μ] and Dominique Damour[†]. The authors would like to thank Anne Dagallier[‡] and Hélène de Foucauld[‡] for modeling studies and Jacques Dumas[μ] and Francis Duffieux[μ] for proofreading.

ABBREVIATIONS USED

HGF, Hepatocyte Growth Factor; NSCLC, Non-Small Cell Lung Cancer; CRC, Colorectal Cancer; PK/PD, Pharmacokinetic/Pharmacodynamic; DFG, Asp-Phe-Gly; ITC, Isothermal Titration Calorimetry; HPLC, High Performance Liquid Chromatography; MW, Molecular Weight; AUC, Area Under the Curve; MSD, Meso Scale Discovery; CV, coefficient of variation

REFERENCES:

(1) Trusolino, L.; Bertotti A.; Comoglio PM. MET signaling: principles and functions in development, organ regeneration and cancer. *Nat. Rev. Mol. Cell Biol.* **2010**, *11*, 834-848.

(2) Guerardi E.; Birchmeier W.; Birchmeier C.; Vande Woude G. Targeting MET in cancer: rationale and progress. *Nature Reviews Cancer* **2012**, *12*, 89-103.

(3) Bladt, F.; Riethmacher, D.; Isenmann, S.; Aguzzi, A.; Birchmeier, C. Essential role for the c-met receptor in the migration of myogenic precursor cells into the limb bud. *Nature* **1995**, *376*, 768-771.

(4) Huh, C.G.; Factor, V.M.; Sánchez, A.; Uchida, K.; Conner, E.A.; Thorgeirsson, S.S. Hepatocyte growth factor/c-met signaling pathway is required for efficient liver regeneration and repair. *Proc. Natl. Acad. Sci. U S A* **2004**, *101(13)*, 4477-4482.

(5) Borowiak, M.; Garratt, A.N.; Wüstefeld, T.; Strehle, M.; Trautwein, C.; Birchmeier, C. Met provides essential signals for liver regeneration. *Proc. Natl. Acad. Sci. U S A* **2004,** *101(29)*, 10608-10613.

(6) Schmidt, L.; Duh, FM.; Chen, F.; Kishida, T.; Glenn, G.; Choyke, P.; Scherer, SW.; Zhuang, Z.; Lubensky, I.; Dean, M.; Allikmets, R.; Chidambaram, A.; Bergerheim, UR.; Feltis, JT.; Casadevall, C.; Zamarron, A.; Bernues, M.; Richard, S.; Lips, CJ.; Walther, MM.; Tsui, LC.; Geil, L.; Orcutt, ML.; Stackhouse, T.; Lipan, J.; Slife, L.; Brauch, H.; Decker, J.; Niehans, G.; Hughson, MD.; Moch, H.; Storkel, S.; Lerman, MI.; Linehan, WM.; Zbar, B. Germline and somatic mutations in the tyrosine kinase domain of the MET proto-oncogene in papillary renal carcinomas. *Nature Genetics* **1997**; *16(1)*, 68-73.

(7) Kong-Beltran, M.; Seshagiri, S.; Zha, J.; Zhu, W.; Bhawe, K.; Mendoza, N.; Holcomb, T.; Pujara, K.; Stinson, J.; Fu, L.; Severin, C.; Rangell, L.; Schwall, R.; Amler, L.; Wickramasinghe, D.; Yauch, R. Somatic mutations lead to an oncogenic deletion of Met in lung cancer. *Cancer Res.* **2006**, *66(1)*, 283-289.

(8) Capuzzo, F.; Marchetti, A.; Skokan, M.; Rossi, E.; Gajapathy, S.; Felicioni, L.; Del Grammastro, M.; Sciarrotta, MG.; Buttitta, F.; Incarbone, M.; Toschi, L.; Finocchiaro, G.; Destro, A.; Terracciano, L.; Roncalli, M.; Alloisio, M.; Santoro, A.; Varella-Garcia, M. Increased MET gene copy number negatively affects survival of surgically resected non-small cell lung cancer patients. *J. Clin. Oncol.* **2009**, *27(10)*, 1667-1674.

(9) Engelman, J.A.; Zejnullahu, K.; Mitsudomi, T.; Song, Y.; Hyland, C.; Park, J.O. ; Lindeman, N. ; Gale, CM.; Zhao, X. ; Christensen, J. ; Kosaka, T. ; Holmes, AJ.; Rogers, AM.; Cappuzzo, F. ; Mok, T. ; Lee, C. ; Johnson, BE.; Cantley, LC. ; Jänne, PA. MET amplification leads to gefitinib resistance in lung cancer by activating ERBB3 signaling. *Science* **2007**, *316*, 1039-1043.

(10) Bean, J.; Brennan, C.; Shih, J.Y.; Riely, G.; Viale, A.; Wang, L.; Chitale, D.; Motoi, N.; Szoke, J.; Broderick, S.; Balak, M.; Chang, WC.; Yu, CJ.; Gazdar, A.; Pass, H.; Rusch, V.; Gerald, W.; Huang, SF.; Yang, PC.; Miller, V.; Ladanyi, M.; Yang, CH.; Pao, W. MET amplification occurs with or without T790M mutations in EGFR mutant lung tumors with acquired resistance to gefitinib or erlotinib. *Proc. Natl. Acad. Sci. U S A* **2007**, *104*, 20932-20937.

(11) Sequist, L.V.; Waltman, B.A.; Dias-Santagata, D.; Digumarthy, S.; Turke, A.B.; Fidias, P.; Bergethon, K.; Shaw, AT.; Gettinger, S.; Cosper, AK.; Akhavanfard, S.; Heist, RS.; Temel, J.; Christensen, JG.; Wain, JC.; Lynch, TJ.; Vernovsky, K.; Mark, EJ.; Lanuti, M.; Iafrate, AJ.; Mino-Kenudson, M.; Engelman, JA. Genotypic and histological evolution of lung cancers acquiring resistance to EGFR inhibitors. *Sci. Transl. Med.* **2011**, *3*, 75ra26.

(12) Bardelli, A.; Corso, S.; Bertotti, A.; Hobor, S.; Valtorta, E.; Siravegna, G.; Sartore-Bianchi, A.; Scala, E.; Cassingena, A.; Zecchin, D.; Apicella, M.; Migliardi, G.; Galimi, F.; Lauricella, C.; Zanon, C.; Perera, T.; Veronese, S.; Corti, G.; Amatu, A.; Gambacorta, M.; Diaz, LA;. Sausen, M.; Velculescu, VE.; Comoglio, P.; Trusolino, L.; Di Nicolantonio, F.; Giordano, S. ; Siena, S. Amplification of the MET receptor drives resistance to anti-EGFR therapies in colorectal cancer. *Cancer Discovery* **2013**, *3*, 658-673.

(13) Straussman, R.; Morikawa, T.; Shee, K.; Barzily-Rokni, M.; Qian, Z.R.; Du, J.; Davis, A.; Mongare, M.M.; Gould, J.; Frederick, D.T.; Cooper, Z.A.; Chapman, P.B.; Solit, D.B.; Ribas, A.; Lo, R.S.; Flaherty, K.T.; Ogino, S.; Wargo, J.A.; Golub, T.R. Tumour micro-environment elicits innate resistance to RAF inhibitors through HGF secretion. *Nature* **2012**, *487*, 500-504.

(14) Liu, X.; Wang, Q.; Yang, G.; Marando, C.; Koblish HK.; Hall, LM.; Fridman, JS.; Behshad, E.; Wynn, R.; Li, Y.; Boer, J.; Diamond, S.; He, C.; Xu, M.; Zhuo, J.; Yao, W.; Newton, RC.; Scherle, PA.

A novel kinase inhibitor, INCB28060, blocks c-MET-dependent signaling, neoplastic activities, and cross-talk with EGFR and HER-3. *Clin. Cancer Res*. **2011**, *17*, 7127-7138.

(15) Bladt, F.; Faden, B.; Friese-Hamim, M.; Knuehl, C.; Wilm, C.; Fittschen, C.; Gradler, U.; Meyring, M.; Dorsch, D.; Jaehrling, F.; Pehl, U.; Stieber, F.; Schadt, O.; and Blaukat, A. EMD 1214063 and EMD 1204831 constitute a new class of potent and highly selective c-Met inhibitors. *Clin. Cancer Res*. **2013**, *19*, 2941-2951.

(16)Jia, H.; Dai, G.; Weng, J.; Zhang, Z.; Wang, Q.; Zhou, F.; Jiao, L.; Cui, Y.; Ren, Y.; Fan, S.; Zhou, J.; Qing, W.; Gu, Y.; Wang, J.; Sai, Y.; Su, W. Discovery of (S)-1-(1-(imidazo[1,2- a]pyridin-6-yl)ethyl)-6-(1-methyl-1 H -pyrazol-4-yl)-1 H -[1,2,3]triazolo[4,5- b]pyrazine (volitinib) as a highly potent and selective mesenchymal-epithelial transition factor (c-Met) inhibitor in clinical development for treatment of cancer. *J. Med. Chem.* **2014**, *57*, 7577-7589.

(17) Hugues, PE.; Yang, Y.; Rex, K.; Zhang, Y.; Kaplan-Lefko, PJ.; Caenepeel, S.; Moriguchi, J.; Broome, M.; Choquette, D.; Radinsky, R.; Kendall, R.; Coxon, A.; Dussault, I. AMG 337, a novel, potent and selective MET kinase inhibitor, has robust growth inhibitory activity in MET-dependent cancer models. *Cancer Res.* **2014**, *74(19 Suppl)*: Abstract 728.

(18) Okamoto, W.; Okamoto, I.; Arao, T.; Kuwata, K.; Yamaguchi, H.; Sakai, K.; Yanagihara, K.; Nishio, K.; Nakagawa, K. Antitumor action of the MET tyrosine kinase inhibitor Crizotinib (PF-02341066) in gastric cancer positive for MET amplification. *Mol. Cancer Ther*. **2012**, *11*, 1557-1564.

(19) Schio, L.; Nemecek, C.; Ugolini, T.; Wentzler, S.; Grapinet, S.; Khider, J.; Albert, E.; Dischamps, N.; Gay, F.; Sonnefraud, V.; Bacqué, E.; Kenigsberg, M.; Goulaouic, H.; Dagallier, A.; Vallée, F.; Bonche, F.; Lengauer, C. SAR125844: a potent and selective ATP-competitive inhibitor of MET kinase. *Cancer Res.* **2012**, *72(8 Suppl 1)*: Abstract 2911.

(20) Egile, C.; Kenigsberg, M.; Delaisi, C.; Begassat, F.; Do-Vale, V.; Mestadier, J.; Bonche, F.; Benard, T.; Nicolas, J.P.; Valence, S.; Lefranc, C.; Francesconi, E.; Castell, C.; Lefebvre, A.M.; Nemecek, C.; Calvet, L.; Goulaouic, H. The selective intravenous inhibitor of the MET tyrosine kinase SAR125844 inhibits tumor growth in MET-amplified cancer. *Mol. Cancer Ther*. **2015**, *14*, 384-394.

(21) Zhao, Z.; Wu, H.; Wang, L.; Liu, Y.; Knapp, S.; Liu, Q.; Gray N. S. Exploration of type II binding mode: a privileged approach for kinase inhibitor focused drug discovery. *ACS Chem. Biol.* **2014**, *9,* 1230-1241.

(22) a).Boezio, A.A.; Copeland, K.W.; Rex, K.; Albrecht, B.K.; Bauer, D.; Bellon, S.F.; Boezio, C.; Broome, M.A.; Choquette, D.; Coxon, A.; Dussault, I.; Hirai, S.; Lewis, R.; Lin, M-H.J.; Lohman, J.; Liu, J.; Peterson, E.A., Potashman, M.; Shimanovich, R.; Teffera, Y.; Whittington, D.A.; Vaida, K.R.; Harmange, J-C. Discovery of (R)‐6-(1-(8-fluoro-6-(1-methyl‐1H‐pyrazol-4-yl)-[1,2,4]triazolo[4,3‐a]pyridin-3-yl)ethyl)-3-(2-ethoxyethoxy)-1,6-naphthyridin-5(6H)‐one (AMG 337), a potent and selective inhibitor of MET with high unbound target coverage and robust in vivo antitumor activity. *J. Med.Chem.* **2016**, *59(6)*, 2328-2342. b). Lolkema, M.P.; Bohets, H.H.; Arkenau, H.T.; Lampo, A.; Barale, E.; de Jonge, M.J.; van Doorn, L.; Hellemans, P.; de Bono, J.S.; Eskens, F.A. The c-Met tyrosine kinase inhibitor JNJ-38877605 causes renal toxicity through species-specific insoluble metabolite formation. *Clin. Cancer Res.* **2015,** *21(10)*, 2297-304.c). Buchanan, S.G.; Hendle, J.; Lee, P.S.; Smith, C.R.; Bounaud, P.Y.; Jessen, K.A.; Tang, C.M.; Huser, N.H.; Felce, J.D.; Froning, K.J.; Peterman, M.C.; Aubol, B.E.; Gessert, S.F.; Sauder, J.M.; Schwinn, K.D.; Russell, M.; Rooney, I.A.; Adams, J.; Leon, B.C.; Do, T.H.; Blaney, J.M.; Sprengeler, P.A.; Thompson, D.A.; Smyth, L.; Pelletier, L.A.; Atwell, S.; Holme, K.; Wasserman, S.R.; Emtage, S.; Burley, S.K.; Reich, S.H. SGX523 is an exquisitely selective, ATP-competitive inhibitor of the MET receptor tyrosine kinase with antitumor activity in vivo. *Mol. Cancer Ther.* **2009**, *8(12)*, 3181-90.

(23) Kawasaki, Y.; Freire E. Finding a better path to drug selectivity. *Drug Discovery Today*, **2011**, *16*, 985-990.

(24) Bissantz, C.; Kuhn, B.; Stahl, M. A medicinal chemist's guide to molecular interactions. *J. Med. Chem.* **2010**, *53*, 5061-5084.

(25) Kornev, A.P; Nina M; Haste, N.M.; Taylor, S.S.; Eyck, L.F.T. Surface comparison of active and inactive protein kinases identifies a conserved activation mechanism. *Proc. Natl. Acad. Sci.*, **2006**, *107*, 17783-17788.

(26) Novel 6-triazolopyridazinesulfanyl benzothiazole and benzimidazole derivatives, method for production thereof and application as medicaments and pharmaceutical compositions and novel use as MET inhibitors (Applicant: Sanofi-Aventis Fr.). Eva Albert, Eric Bacque, Conception Nemecek, Antonio Ugolini, Sylvie Wentzler. WO2009056692 A2; May 7, 2009.

(27) Leeson, P.D.; Young, R.J. Molecular property design: does everyone get it? *ACS Med. Chem. Lett.* **2015**, *6*, 722-725.

(28) Veber, D. F.; Johnson, S. R.; Cheng, H.-Y.; Smith, B. R.; Ward, K. W.; Kopple, K.D. Molecular properties that influence the oral bioavailability of drug candidates. *J. Med.Chem.* **2002**, *45*, 2615-2623.

(29) Doak, B. C.; Zheng, J.; Dobritzsch, D.; Kihlberg, J. How beyond rule of 5 drugs and clinical candidates bind to their targets. *J. Med.Chem.* **2016**, *59(6)*, 2312-2327.

(30) a). Derivatives of 6-(6-O-cycloalkyl or 6-NH-cycloalkyl-triazolopyridazine-sulfanyl) benzothiazoles and benzimidazoles, preparation thereof, use thereof as drugs, and use thereof as MET inhibitors. (Applicant: Sanofi-Aventis Fr.); Eric Bacque, Conception Nemecek, Antonio Ugolini, Sylvie Wentzler; WO2010089506 A1; Aug 12, 2010. b). Derivatives of 6-(6-O-substituted-triazolopyridazine-sulfanyl) benzothiazoles and benzimidazoles, preparation thereof, use thereof as drugs, and use thereof as MET inhibitors (Applicant: Sanofi-Aventis Fr.); Conception Nemecek, Antonio Ugolini, Sylvie Wentzler; WO2010089507 A1; Aug 12, 2010. c). Derivatives of 6-(6-NH-substituted-triazolopyridazine-sulfanyl) benzothiazoles and benzimidazoles, preparation thereof, use thereof as drugs, and use thereof as MET inhibitors (Applicant: Sanofi-Aventis Fr.); Eric Bacque, Conception Nemecek, Antonio Ugolini, Sylvie Wentzler; WO2010089508 A1; Aug 12, 2010.

(31) Angevin, E.; Spitaleri, G.; Hollebecque, A.; De Pas, T.; Soria, J.C.; Harnois, M.; Mazuir, F. ; Assadourian, S.; De Marinis, F. A first-in-human (FIH) phase I study of SAR125844, a novel selective

MET kinase inhibitor, in patients (pts) with advanced solid tumors: Dose escalation results. *J. Clin. Oncol.* **2014**, *32(5 Suppl)*: Abstract 2506.

Graphic for Table of Contents Only: